Inelastic Scattering in Reflection High-Energy Electron Diffraction from Si(111)

Bert Müller and Volkmar Zielasek

Institut für Festkörperphysik, Universität Hannover, Appelstrasse 2, D-30167 Hannover, Germany, and Institut für Quantenelektronik, Eidgenössische Technische Hochschule Zürich, CH-8093 Zürich, Switzerland

(Received 10 July 1997)

Inelastic electron scattering from Si(111) is investigated by high-resolution, energy-filtered reflection high-energy electron diffraction. We demonstrate that plasmon excitation and electron-hole generation result in a characteristic spot broadening which is properly described by dipole scattering theory. Moreover, we found evidence for reduced coherence of the dipole scattered electrons. Diffraction spots broadened due to surface roughness and inelastic scattering can have identical shape. Consequently separation is possible only by combining high angular and energy resolution. [S0031-9007(97)04722-4]

PACS numbers: 61.14.Hg, 68.35.Bs, 73.20.Mf, 81.15.Hi

Electrons are the strong scattering probes of choice to characterize crystalline surfaces on atomic scale. Reflection high-energy electron diffraction (RHEED) has provided a wealth of information on the microscopic structure of an enormous variety of systems [1]. The analysis of electron diffraction experiments is usually limited to elastic scattering, i.e., to zero-energy transfer, which is, in fact, a special case. Energy losses ranging from a tenth of millielectronvolts to hundreds of electronvolts, which are the focus of several surface sensitive techniques, are generally ignored in RHEED pattern interpretations [2]. Elastic scattering is believed to appear very intense and confined to certain angles, whereby inelastic scattering is often attributed as weak and diffuse. Essential technical improvements achieved only very recently allow us to demonstrate the significance of plasmon scattering in RHEED. In the case of silicon, the observed Kikuchi features result from plasmon scattering [3,4], and the clear appearance of the shadow edge is due to increased plasmon scattering nearby the edge [5]. However, a clear understanding of the influence of inelastic scattering on the RHEED pattern is still lacking. This is a prerequisite for a reliable determination of surface morphology from spot profiles as performed with much success in low-energy electron diffraction (LEED) [6]. With respect to low-energy electrons and almost normal incidence, the grazing incidence in RHEED has many advantages, e.g., the comfortable geometry for growth studies and the substantially improved momentum resolution perpendicular to the shadow edge.

In the present Letter we demonstrate the dramatic effect of inelastic scattering on the spot profiles. The dipole scattering theory [7] adequately describes the spot broadening in grazing incidence electron diffraction for primary energies between 4 and 10 keV. In comparison with typical RHEED experiments, this energy range is better regarded as medium. Both medium energy electron diffraction and RHEED are characterized by forward scattering but the total cross section of the inelastic dipole scattering scales by the inverse of the square root of the primary energy [8]. Hence dipole scattering effects are more pronounced in the present study than in conventional RHEED studies. Besides the surface plasmon excitation as a dominant inelastic process [9–11] we have identified electron-hole generation across the direct band gap as additional dipole loss.

Our unique high-resolution, energy-filtered RHEED system [12] providing an angular resolution of 0.1 mrad and an energy resolution of 4 eV is especially suitable for the investigation of elastic and inelastic spot profiles. Energy filtering is done by adjusting the retarding field in front of the detector (channeltron). The energy of the incident electron beam is stabilized to less than 1 eV. The highly oriented Si(111) samples were heated by direct current up to about 1200 °C to remove the oxide and some of the outermost layers. This procedure results in a perfect (7×7)-reconstructed surface. The RHEED measurements were performed at room temperature and at a total pressure always below 2×10^{-8} Pa.

The influence of inelastic scattering on the RHEED spots is found qualitatively as a formation of a broad halo around each spot, which is slightly extended in the direction parallel to the shadow edge (see Fig. 1). The spot profiles taken in this direction exhibit not only the sharp elastic peak but also include a symmetric broadening of each spot designated "shoulder." The peak intensity and half-width of this shoulder depend on the retarding field of the energy filter. This shoulder is apparently formed by the inelastically scattered electrons and can be easily distinguished from the central elastic spike. The sharpness of this spike yields a mean terrace width of 200 nm (out-of-phase condition for the specular beam in Fig. 1, i.e., electrons scattered from adjacent surface terraces interfere destructively). The shoulder including energy losses up to $\Delta E = 12$ eV is mainly due to single surface plasmon excitations [5]. The surface plasmon energy is 10.8 eV [13]. The broader shoulder for ΔE up to 66 eV includes also multiple surface and bulk plasmon losses. The profile taken by our special detection unit for $\Delta E = 66$ eV is almost identical to the one reproduced from a fluorescent screen of a conventional RHEED system. The

ratio between the integral elastic and inelastic intensity of the specular beam at $E = 4644$ eV and incident angle $\alpha = 2.65°$ corresponds to 0.02. For more grazing incidence the ratio becomes even smaller, e.g., at $\alpha = 0.7°$ we have found 0.002 [5]. This means that most of the diffracted electrons in RHEED undergo plasmon losses and are visible not only as shadow edge and Kikuchi features but also as halos around each spot. Reflection high-energy electron loss spectroscopy shows only minor effects due to bulk plasmons on Si(111) [9,14]. For surface plasmon excitations, dipole scattering theory is expected to provide an adequate description of electron scattering [7]. In dipole fields, set up in the vacuum above the surface by charge-density fluctuations in the surface, electrons are scattered nearly in forward direction. The scattering process takes place at a characteristic distance $d \approx 1/K_{||}$ from the surface, with $K_{||} = |(\mathbf{k}_F - \mathbf{k}_I)_{||}|$ as scattering vector component parallel to the surface where $\mathbf{k}_I$ and $\mathbf{k}_F$ are momentum of incident and scattered electrons, respectively. For incident energies up to several keV and energy losses higher than the band gap, retardation effects can be neglected [15]. The angular distribution $dS/d\Omega$ for a specific dipole loss ΔE is like a lobe around the specular reflection:

$$\frac{dS}{d\Omega} \sim \frac{1}{\sin\alpha} \frac{\sqrt{(\Delta E/2E\cos\alpha - \vartheta\sin\alpha\cos\varphi)^2 + \vartheta^2\sin^2\varphi}}{[\vartheta^2 + (\Delta E/2E)^2]^2}.$$

Here $\sim$ denotes proportionality and, according to Fig. 2, α is the angle of incidence, ϑ is the scattering angle, and φ the scattering azimuth. Using $\cos\alpha \approx 1$ because of the grazing incidence we obtain a Lorentzian profile with exponent 3/2 parallel to the shadow edge, i.e., $dS/d\Omega(\varphi = \pi/2) \sim 1/\{\vartheta^2 + [\Delta E/(2E)]^2\}^{3/2}$ [16].

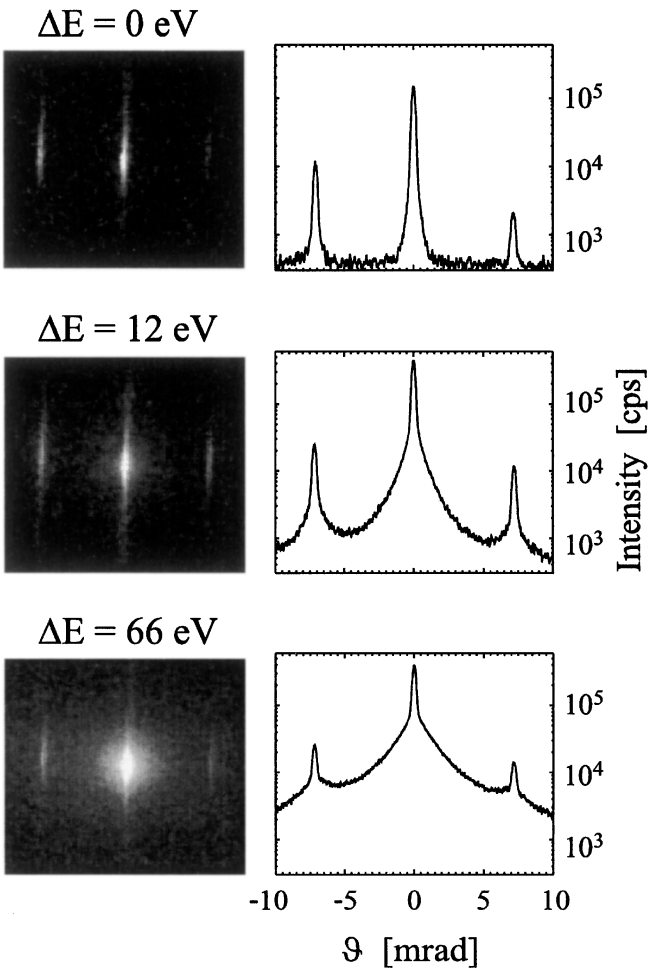

FIG. 1. Inelastic halo in the RHEED pattern and corresponding profiles of specular and 1/7 spots of the 0. Laue circle for Si(111)-(7 × 7) in $[01\bar{1}]$ azimuth at $E = 4644$ eV and $\alpha = 2.65°$. $\Delta E = 0$ means that only elastically scattered electrons are detected. The other pattern includes losses up to 12 and 66 eV, respectively.

Shape and half-width of the angular distribution depend only on the scattering geometry and the ratio of energy loss and primary energy. The inelastic part of the profiles as expected for the single surface plasmon loss is shown as the black colored region in Fig. 3. Not only the scattering geometry but also the finite momentum resolution due to instrumental limits and surface defects has been taken into account by convoluting the dipole lobe with the experimental elastic profile. In order to care for the full width at half maximum of the surface plasmon loss (8.8 eV) [13], $dS/d\Omega$ has been integrated with respect to ΔE using a Gaussian distribution (the result is almost identical to a discrete loss at 10.8 eV). The profiles in Fig. 3 include losses up to 20 eV so that the detected intensity fully comprises single plasmon scattering. The only fit parameter is the intensity, i.e., the total plasmon scattering cross section.

The major part of the inelastic shoulder can be explained as due to single surface plasmon scattering. Additional intensity in the inelastic shoulder visible in the experimental data near the elastic spike gives evidence for another inelastic process associated with lower energy

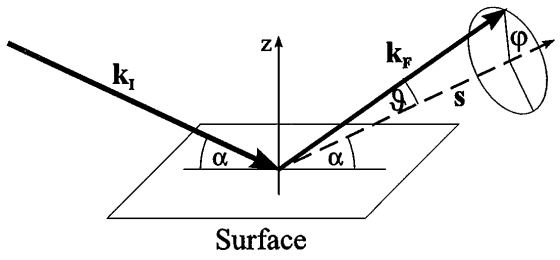

FIG. 2. Scattering geometry in RHEED illustrating angle of incidence α, scattering angle ϑ, and scattering azimuth φ. $\mathbf{k}_I$ and $\mathbf{k}_F$ denote the momentum of incident and scattered electrons, respectively.

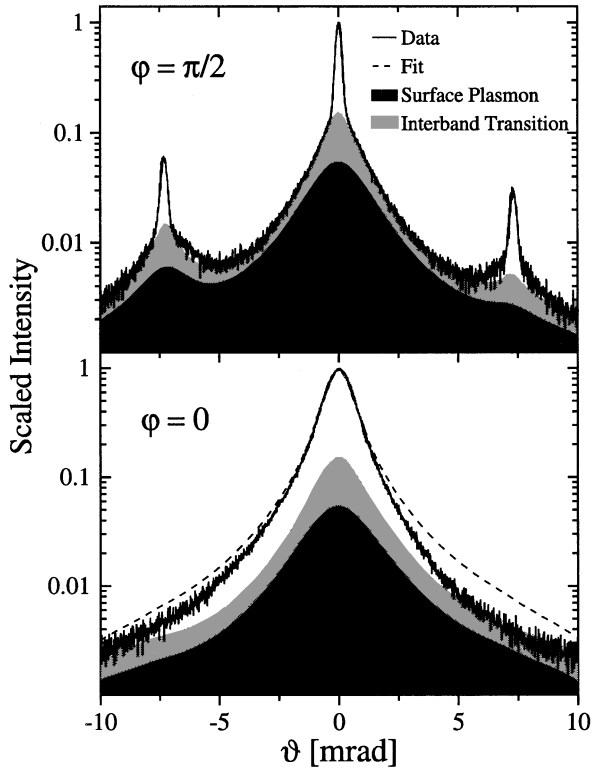

FIG. 3. Profiles through specular beam as shown in Fig. 1 despite $\Delta E = 20$ eV parallel to shadow edge (upper part) and perpendicular to shadow edge (lower part) fitted with a Gaussian (elastic scattering) and inelastic dipole scattering of surface plasmon and interband transition at Γ. The experimental data are represented by a solid line, fits by a dashed lines. In the upper part both experiment and fit are identical. Inelastic scattering due to surface plasmons and interband transitions are shown as black and gray areas, respectively.

but minor total intensity. According to the equation mentioned above, the width of the inelastic halo is proportional to the energy loss ΔE. Indeed, the optical response of semiconductors exhibits absorption maxima between the band gap and 6 eV due to interband transitions [17]. We performed a fit assuming an additional loss using not only the total loss intensities as fit parameters but also the second loss energy. The fitting procedure leads to $\Delta E = 3.4 \pm 0.3$ eV (gray colored in Fig. 3), a value which corresponds to the direct gap between the topmost valence band and the lowest conduction band at the Γ point of reciprocal space [18]. The two dipole losses perfectly describe the inelastic shoulder of the spot profile parallel to the shadow edge so that any deviation between experiment and fit cannot be seen in Fig. 3 ($\varphi = \pi/2$).

Perpendicular to the shadow edge ($\varphi = 0$), the momentum resolution parallel to the surface is increased due to grazing incidence by $1/\sin\alpha$ and the elastic spike is usually broadened by 1 or 2 orders of magnitude. In this direction the inelastic scattering does not produce any separate shoulder if the specular beam is near out of phase (Fig. 3, $\varphi = 0$). Indeed, shape and half-width of the profile remain almost unaffected by a variation of the retarding potential of the energy filter. Nevertheless, the dipole scattering theory fits also perpendicular to the shadow edge. The black and gray colored areas denote the inelastic profile as expected in this direction due to the fit result obtained parallel to the shadow edge. The difference of the experimental data and the inelastic profile should represent elastic scattering and has been fitted by the experimental elastic profile (energy filter set to $\Delta E = 0$). The result (dashed line) and the experimental data agree fairly well within ± 5 mrad. The kinematic approximation delivers a proper description of the profile although one would assume remarkable changes along the Bragg rod as found in rocking curve measurements due to dynamic effects. Surprisingly, the agreement between fit and experiment outside the center of the profile is also quite good. Corresponding results have been obtained for various angles of incidence (0.7°–7.4°). We have not observed electron surface channeling effects as described for GaAs [19] which might give rise to significant intensity from inelastic scattering in the topmost surface layers. This means that the dipole scattering theory perfectly describes the spot broadening due to plasmon losses and interband transitions.

By means of the profiles parallel to the shadow edge for our samples with an average terrace size of 200 nm one can clearly separate elastic and inelastic contributions in the RHEED pattern. Thus, rocking curves, i.e., the intensity vs angle of incidence, for the elastic and inelastic scattering can be compared (Fig. 4). The data are the one dimensionally integrated intensities of the profiles parallel to the shadow edge. The angle of incidence is presented in Fig. 4 as a relative scattering phase of adjacent surface terraces in units of 2π. The inelastic curve is scaled by $\sin\alpha$ in order to eliminate the dependency of the total dipole scattering cross section of single losses on the angle of incidence. At phase 2.4, both rocking curves exhibit a maximum due to the (333) bulk Bragg spot [3]. Contrary to the inelastic rocking curve, the elastic rocking curve, however, exhibits maxima at in-phase conditions, i.e., constructive interference from adjacent terraces. Therefore, these maxima occur due to the surface roughness. Since we integrate only in the direction of low resolution we are still sensitive to the spike intensity because of the high momentum resolution perpendicular to the shadow edge. The spike intensity is closely related to the vertical surface roughness. For the present multilevel system, i.e., the surface consists of terraces on many atomic levels, the elastic profile broadens outside the in-phase condition by formation of a shoulder. Hence, maxima of the elastic rocking curve are observed at in-phase.

These maxima are not observed for the inelastic rocking curve because the coherence is reduced by the immense beam divergence due to the dipole scattering. The divergence of the electron beam caused by surface plasmon

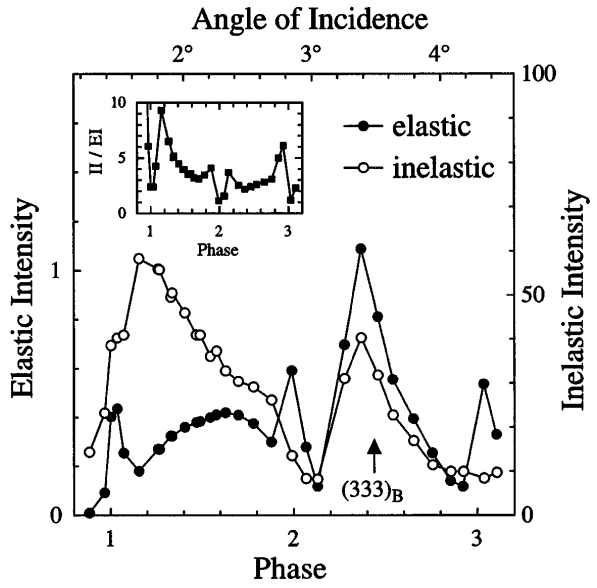

FIG. 4. Rocking curves of integral intensities for elastically and inelastically scattered electrons, respectively. Note, the different scaling. Inset: ratio of II and EI vs phase (angle of incidence). EI denotes the integral elastic intensity and II the integral inelastic intensity scaled by $\sin\alpha$ to eliminate the dependence of the total dipole scattering cross section of single losses on the angle of incidence.

scattering corresponds to more than 3 mrad (primary energy 6 kV), a value which is about 2 orders of magnitude higher than that of the primary beam of our instrument. That means, a correlation length larger than 60 nm is not detectable by the inelastically scattered electrons [20]. Here, the surface appears totally flat and the inelastic rocking curve shows no in-phase maxima because the average step distance is 200 nm. It should be mentioned that the inelastic rocking curve corresponds to conventional rocking curves because the inelastic intensity dominates [3].

The inelastic shoulder might be misinterpreted as due to surface roughness. At in-phase condition the relative inelastic intensity is reduced because of the elastic maxima. This is obvious in the inset of Fig. 4 showing the inelastic intensity related to the elastic intensity. Therefore, the shoulder due to inelastic scattering shows the same phase dependence like a shoulder due to surface roughness. More seriously, their shape can be identical. As an example, the morphology of a two-level system produces a Lorentzian shoulder with exponent $3/2$ [21] as found here for the inelastic profile parallel to the shadow edge. Thus, a precise spot profile analysis is feasible only by means of an energy-filtered instrument [22]. Rough estimates of average terrace sizes can be obtained from profiles perpendicular to the shadow edge when the specular beam is out of phase [20]. With a simple retarding energy filter, however, RHEED can yield quantitative information on surface morphology and on electronic surface structure and film composition of growing surfaces on atomic scale simultaneously.

We gratefully acknowledge financial support by the Volkswagen-Stiftung, Germany, and the Karl Sulzberger-Fond, Switzerland. It is our pleasure to thank our tutor M. Henzler for his indispensable support and help.

[1] P. K. Larsen and P. J. Dobsen, *Reflection High-Energy Electron Diffraction and Reflection Electron Imaging of Surfaces*, NATO ASI Ser. B, Vol. 188 (Plenum, New York, 1988).
[2] An exception is given by H. A. Atwater *et al.* They routinely perform chemical analysis by measurement of core losses in RHEED; see, e.g., H. A. Atwater and C. C. Ahn, Appl. Phys. Lett. **58**, 269 (1991).
[3] Y. Horio, Jpn. J. Appl. Phys. **35**, 3559 (1996).
[4] D. E. Savage and M. G. Lagally (private communication).
[5] B. Müller, VDI Research Report No. 9/197, 1994.
[6] M. Henzler, Appl. Phys. A **34**, 205 (1984).
[7] H. Ibach and D. L. Mills, *Electron Energy Loss Spectroscopy and Surface Vibrations* (Academic Press, New York, 1982).
[8] H. Froitzheim, in *Electron Spectroscopy for Surface Analysis*, edited by H. Ibach (Springer, Berlin, 1977).
[9] O. L. Krivanek *et al.*, Ultramicroscopy **11**, 215 (1983).
[10] A. Howie, Ultramicroscopy **11**, 141 (1983).
[11] L.-M. Peng *et al.*, Phys. Lett. A **175**, 461 (1993).
[12] B. Müller and M. Henzler, Rev. Sci. Instrum. **66**, 5232 (1995).
[13] H. Raether, *Excitations of Plasmons and Interband Transitions by Electrons* (Springer-Verlag, Berlin, 1980).
[14] Y. Horio *et al.*, Appl. Surf. Sci. **101**, 292 (1996).
[15] R. Garcia-Molina *et al.*, J. Phys. C **18**, 5335 (1985).
[16] Note, for small α the intensity is distributed nearly symmetrically around the specular reflection but the wave vector components perpendicular to the shadow edge of the excited surface plasmons are confined to values very near to $\sqrt{2mE}(1 - \sqrt{1 - \Delta E/E})\cos\alpha$ due to the scattering geometry.
[17] H. R. Philipp and H. Ehrenreich, Phys. Rev. **129**, 1550 (1963).
[18] Landolt-Börnstein, *Neue Serie* (Springer-Verlag, Berlin, 1987), Vol. III/22a, p. 14.
[19] Z. L. Wang, Surf. Sci. **214**, 44 (1989).
[20] B. Müller and V. Zielasek (to be published).
[21] C. S. Lent and P. I. Cohen, Surf. Sci. **139**, 121 (1984).
[22] B. Müller and M. Henzler, Surf. Sci. (to be published).